Draft version August 9, 2004
Preprint typeset using LaTeX style emulateapj v. 11/12/01

XMM-NEWTON OBSERVATION OF THE DOUBLE PULSAR SYSTEM J0737–3039

Sergio Campana
INAF-Osservatorio Astronomico di Brera, Via Bianchi 46, I–23807 Merate (Lc), Italy

Andrea Possenti, Marta Burgay
INAF-Osservatorio Astronomico di Cagliari, Loc. Poggio dei Pini, Strada 54, I–09012 Capoterra (Ca), Italy
Draft version August 9, 2004

ABSTRACT

We report on a 50 ksec XMM-Newton observation of the double pulsar system J0737–3039 performed on April 2004. We present results of the spectral analysis of these data combined with the much shorter Chandra pointing performed on January 2004. Black body emission with effective temperature of $0.20^{+0.02}_{-0.02}$ keV (90% confidence level) and emission radius 75^{+30}_{-9} m for a distance of 0.5 kpc (implying a 0.5–10 keV luminosity $\sim 6 \times 10^{29}$ erg s^{-1}) is a viable interpretation, calling for a stream of particles accelerated in the magnetosphere of PSR J0737–3039A and depositing their kinetic energy in the magnetic polar cap of PSR J0737–3039A or of the companion PSR J0737–3039B. A single power-law emission model implies a very steep photon index $\Gamma = 4.2^{+2.1}_{-1.2}$ and a suspiciously high hydrogen column density, whereas a photon index $\Gamma = 2$ does not provide an adequate description of the XMM-Newton and Chandra data. A two component model (a black body plus a power-law with $\Gamma = 2$) is statistically acceptable, but the additional power-law component is not required by the data.

Subject headings: stars: neutron — pulsars: individual (PSR J0737–3039A, PSR J0737–3039B) — X–rays: stars — radiation mechanisms: thermal, non-thermal

1. INTRODUCTION

PSR J0737–3039A/B (Burgay et al. 2003; Lyne et al. 2004) is the first double pulsar ever known. It comprises a 22-ms pulsar (PSR J0737–3039A, hereafter A) and a 2.7-sec pulsar (PSR J0737–3039B, hereafter B) revolving in 2.4 hr about the common center of mass along a mildly eccentric ($e = 0.09$) and highly inclined ($\sim 87^\circ$) orbit. These orbital parameters ensure a large magnitude for several post-keplerian parameters, making this binary an unprecedented test-bed for theories of gravity and relativistic physics (Lyne et al. 2004; Kramer et al. 2004).

Further unique features of J0737–3039 double neutron star system are the occurrence of both an eclipse of A's radio signal at superior conjunction (Lyne et al. 2004; Kaspi et al. 2004) and a modulation of flux and pulse shape of pulsar B along the orbit (Lyne et al. 2004; Manchester et al. 2004; Ramachandran et al. 2004). These phenomenologies are signatures of the interaction between the relativistic wind from A (releasing a spin-down power $\dot{E}_A = 5.8 \times 10^{33}$ erg s^{-1}, 3600 times larger than $\dot{E}_B$) and B's magnetosphere and open the possibility of shedding light on still unanswered issues related with neutron star magnetosphere, pulsar winds and coherent radio emission (Lyutikov 2004; Arons et al. 2004; Jenet & Ransom 2004).

The evidence for strong interactions between relativistic particles from one pulsar and the other's magnetic field immediately triggered interest for observations of the J0737–3039 system in the X–ray band. A short 10 ksec observation with the Chandra ACIS-S instrument resulted in a clear detection of the binary (McLaughlin et al. 2004) with no significant evidence for variability along the orbit on timescale longer than 15 min. The available 77 photons could be represented satisfactorily (McLaughlin et al. 2004) by a power-law spectrum with photon index $\Gamma = 2.9 \pm 0.4$ and $N_H = 4.8^{+3.4}_{-2.4} \times 10^{20}$ cm^{-2} (1σ confidence error) resulting in a 0.2–10 keV luminosity of $2.3^{+0.5}_{-0.4} \times 10^{30}$ erg s^{-1} at the distance of 0.5 kpc, inferred from the pulsars' dispersion measure and a model for the Galactic electron density (Cordes & Lazio 2002). The inferred X–ray luminosity and spectral index are consistent with an emission originating solely from the magnetosphere of pulsar A, but emission from the shocked wind of pulsar A as it interacts with the interstellar medium (or with the magnetosphere of pulsar B) could be another viable hypothesis (Granot & Mészáros 2004).

XMM-Newton targeted J0737–3039 system on April 2004 collecting about three times more photons than the January 2004 Chandra pointing. We here report on the analysis of the XMM-Newton data and present the improved spectral fit made possible by joining the data set of the two observations.

2. XMM-NEWTON OBSERVATION

2.1. *Data collection and reduction*

XMM-Newton observed PSR J0737–3039A/B on 10th April 2004 for 50 ks following an unsolicited target of opportunity request. Data were taken in Full Frame (full image with 2.6 s timing resolution) and Small Window ($\sim 2' \times 2'$ imaging with 0.3 s timing resolution) mode for MOS1 and MOS2, respectively, and with a medium filter. Data from the pn detector were taken in timing mode (1 dimensional imaging and 0.03 ms timing resolution) with a medium filter too. We extracted the event files running `emproc` under SAS v6.0. Analysis of the light curve revealed that a sizable part of the observation was corrupted by soft photon flares. We extracted, from the entire MOS images, a total light curve with binning time of 50 seconds and created a time filter excluding intervals with rate larger than 5 count s^{-1} (e.g. Snowden et al. 2004). The good time intervals amount to 20.5 ks and

25.4 ks for the two MOS cameras, respectively. In the central part of the MOS1 filtered image we can detect (using XIMAGE v4.2) only one source. Its location is fully consistent with that of PSR J0737–3039A/B derived from timing observation (Lyne et al. 2004), with a count rate of $(3.3 \pm 0.5) \times 10^{-3}$ couns s^{-1}. The source turns out to be too faint for a detection with the pn in timing mode and these data were not analysed any further. From the filtered data we extracted the MOS source spectrum (circular region centered on source with $r = 20''$ extraction radius) and the background spectrum (for the MOS1 using an annular region centered on source with inner and outer radii $r_{int} = 40''$ and $r_{ext} = 80''$ respectively, and for the MOS2 using two $r = 20''$ regions near the right corners of the small window image). The background accounts for $\sim 80\%$ and $\sim 65\%$ of the total counts for the MOS1 and MOS2 respectively, which are 81 and 145. We generated response and ancillary files with the latest CCF library and fit together the two spectra. We have also analysed the data collected on 18th January 2004 with the ACIS-S instrument onboard Chandra finding similar results to McLaughlin et al. (2004). In the latter data, the source appears slightly extended (with a $\sim 2\sigma$ statistical significance), but the small number of counts (about 80) does not allow to derive firm conclusions.

2.2. *Spectral fitting*

We tried several emission models to the joint MOS1, MOS2 and Chandra spectra rebinning the data to 20 and 15 photons per channel for the two MOS and the ACIS-S respectively; hence a total of 16 spectral channels, ranging from 0.5 keV up to 10 keV for MOS1 and MOS2 (the photons with energies less than 0.5 keV have been excluded owing to the uncertainties in the calibration of the two MOS cameras) and 0.3–10 keV for the ACIS-S data (corrected for the degradation in the ACIS-S quantum efficiency within XSPEC with the `ACISABS` component). The adopted spectral binning guarantees the proper use of the χ^2 goodness-of-fit evaluator. The spectra have been modelled and fitted using the XSPEC package v.11.3 with an absorption component modelled by `TBABS`.

As reported in Table 1, all the explored single component models are acceptable from the point of view of the goodness-of-fit. However, their physical interpretation is less straightforward. We review these models in the following.

A black body model provides a good fit to the data with a $\chi^2_{red} = 1.6$ (where χ^2_{red} is the reduced χ^2). Given the small number of degree of freedom (12) the null hypothesis probabily (n.h.p.) is 7% (Fig. 1). The black body equivalent temperature is $k\,T_{\rm bb} = 0.20^{+0.02}_{-0.02}$ keV (i.e. $T = 2.5^{+0.04}_{-0.05} \times 10^6$ K; here and in the following we use 90% confidence interval for one interesting parameter, i.e. $\Delta\chi^2 = 2.71$). We can put only an upper limit on the column density $N_H < 0.4 \times 10^{21}$ cm^{-2}. This upper limit is consistent with the neutral hydrogen absorption measured in other sources with similar celestial coordinates and having distance $\lesssim 1$ kpc, as inferred using the ISM Column Density Search Tool [1] and from an estimate from the radio pulsars disperion measures of $N_H = 1.5 \times 10^{20}$ cm^{-2}. The unabsorbed 0.5–10 keV flux is 1.9×10^{-14} erg s^{-1} cm^{-2}, converting into a luminosity of 5.8×10^{29} erg s^{-1}. For the reference distance of 0.5 kpc, the efficiency η of conversion of rotational energy loss $\dot{E}_A$ into 0.5–10 keV luminosity is $\eta \sim 10^{-4}$ and the equivalent black body radius is very small $R_{\rm bb} = 75^{+30}_{-9}$ m. Deriving an emitting radius of few kilometers requires much larger distances for the source, even when adopting neutron star atmosphere models. In particular, fixing the emitting radius to 10 km, the atmospheric emission model `NSA` of the XSPEC package places the source at 13.8 kpc, more than 20 times farther than the distance inferred according to the dispersion measure distance indicator.

A thermal bremsstrahlung model is statistically acceptable too ($\chi^2_{red} = 1.0$, n.h.p. 42%). The equivalent temperature is $k\,T_{\rm br} = 0.56^{+0.18}_{-0.19}$ keV. The column density is $N_H < 1.0 \times 10^{21}$ cm^{-2} The 0.5–10 keV unabsorbed flux is 3.2×10^{-14} erg s^{-1} cm^{-2}. At 0.5 kpc this translates into a luminosity of 9.5×10^{29} erg s^{-1}. The emission measure for the adopted distance is $3.6^{+6.6}_{-1.1} \times 10^{53}$ cm^{-3}. Following Grindlay et al. (2002) we can estimate the plasma density $n \sim 10^{26}\,R^{-3/2}$ cm^{-3} for a spherical region of radius R. Assuming a mean particle density typical of the interstellar medium, i.e. $n = 1$ cm^{-3}, the radius of the emitting region turns out ~ 0.1 pc, much larger than the binary separation. Finally we note that a fit with a Raymond-Smith model provides an unacceptable result in the case of an emitting region of solar metallitiy ($\chi^2_{red} = 4.3$). The upper limit on the abundance is $Z < 0.01\,Z_\odot$.

A power-law model ($\chi^2_{red} = 0.9$, n.h.p. 54%) is characterized by a photon index $\Gamma = 4.2^{+2.1}_{-1.2}$. Given this steep power-law also the column density is very high $N_H = 1.8^{+1.6}_{-0.7} \times 10^{21}$ cm^{-2}, comparable to the full galactic value ($N_H = 4.7 \times 10^{21}$ cm^{-2}) derived from neutral hydrogen measurements (Dickey & Lockman 1990). The unabsorbed 0.5–10 keV flux amounts to 4.7×10^{-14} erg s^{-1} cm^{-2}. Placing PSR J0737–3039A/B at 0.5 kpc, this results in a luminosity of 1.4×10^{30} erg s^{-1}, corresponding to an efficiency $\eta \sim 2 \times 10^{-4}$. We note that a $\Gamma = 2$ model has a null hypothesis probability of 5×10^{-7} (see Fig. 2).

A fit for a multi-components model keeping all the parameters free is not meaningful, owing to the limited total number of available photons and taking in account the reported statistical significance of the fits for the single component models. Given its possible physical relevance (see below), we here only report on a two components model made by a black body plus a power-law with photon index fixed to $\Gamma = 2$. Also in this case we obtained a good description of the data ($\chi^2_{red} = 1.2$, n.h.p. 28%). The black body component parameters are similar to those of the single black body model ($k\,T_{\rm bb} = 0.16 \pm 0.04$ keV, $R_{\rm bb} = 90^{+83}_{-28}$ m). The percentage contribution to the total flux (2.7×10^{-14} erg s^{-1} cm^{-2}) of the power-law component is $\sim 52\%$.

We also attempted a temporal analysis. We folded the MOS light curves to the orbital period without revealing any significant variation accross the orbit with an upper limit of 40% ($3\,\sigma$, see Fig. 3). The aforementioned failure in detecting the source in the pn detector prevented any search of modulation at the spin period of each the two pulsars.

[1] http://archive.stsci.edu/euve/ism/ismform.html

3. DISCUSSION

We have performed a joint spectral analysis of the XMM-Newton and Chandra observations of the J0737-3039 binary system, exploiting a three times larger amount of photons than the Chandra observation only (McLaughlin et al. 2004).

Black body emission seems a viable model. Given the age of the system ($\gtrsim 50$ Myr since the second supernova explosion, Lorimer et al. 2004) the contribution in the 0.5–10 keV band due to the cooling of the two neutron stars is negligible, but thermal emission could be powered by a flow of particles impinging onto the surface of one (or both the) neutron star(s). Pulsar A is likely to provide the required energetic budget as the spin-down power of pulsar B is only 2×10^{30} erg s^{-1} (Lyne et al. 2004). The simplest picture calls for back-flowing of charged particles accelerated in the A's polar gap and depositing their kinetic energy in the A's magnetic polar cap (Cheng & Ruderman 1980; Arons 1981). The observed equivalent emitting radius is tiny, much smaller than the polar cap radius of pulsar A ($r_{\rm pc} \sim 1$ km), but partially filled polar cap thermal emission can be invoked, accounting for emitting radii as small as few tens of meters (Harding & Muslimov 2002). Alternatively, a much larger cap area results from modeling the data with a non-uniform temperature of the heated region (Zavlin et al. 2002). In this picture a sinusoidal X-ray emission at the pulsar A spin period (22.7 ms) is expected.

In fact, a sizable number of millisecond pulsar (MSPs) with black body spectra has been already observed in the field and in globular clusters. In particular thermal contributions and cap radii as small as 30–40 m have been invoked in order to fit the X–ray spectra of the nearby pulsar PSR J0437–4715 (Zavlin et al. 2002) in the galactic field. We also note that the equivalent temperature of the emission from J0737–3039 system (0.2 keV) perfectly matches with the one of the pure black body spectrum of the MSPs observed in 47 Tuc's with Chandra (even if not based on a source by source spectral fits, Grindlay et al. 2002). The X–ray luminosities (and hence the emitting radii) are also comparable, once accounted for the intrinsic uncertainties in the distance of the J0737–3039 system. This agreement is somewhat surprising given the much older ages of the MSPs in 47 Tuc ($>$ few 10^9 yrs, Grindlay et al. 2002) with respect to the extimated time since formation of PSR J0737–3039A.

Alternatively, it is conceivable that a fraction of the A's relativistic stream of particles is intercepted and channeled onto pulsar B polar cap(s) whose radius is $80-90$ m (compatible with the inferred $R_{\rm bb}$ at 95% confidence level). This hypothesis requires that ~ 3% of the spin-down luminosity (supposed isotropically released) of pulsar A powers the observed X–rays. A modulation of the X-ray light curve at the B's spin period (or at a beating frequency between A's and B's rotational periods) is a predictable consequence of this model. A more detailed model along these lines has been presented by Zhang & Loeb (2004). Deeper exposures in small window with the pn instrument aboard XMM-Newton might reveal this modulation or the one at the A's spin period, strongly constraining the origin of X-ray in this binary.

Bremsstrahlung emission requires an emitting region much larger than the binary separation and also larger (by a factor of ~ 100) than the radius of the bow shock between the relativistic wind of pulsar A and the ambient medium for a typical density of 1 atom cm^{-3} (and relative velocity of 200 km s^{-1}, Ransom et al. 2004). This translates in an angular extension of the emitting region of $\sim 1'$ for a distance of 0.5 kpc, which is excluded by both the Chandra and XMM-Newton observations.

Absorbed single power-law emission models have been frequently used for interpreting the X-ray spectra of millisecond pulsars (e.g. Becker & Trümper 1999; Becker & Aschenbach 2002; Nicastro et al. 2004). In this hypothesis the X–ray emission from J0737–3039 system would be ascribed to processes involving particles produced and accelerated in the magnetosphere of pulsar A. However, no MSP with an X–ray power-law spectrum as steep as $\Gamma \gtrsim 3$ is known and a power-law model with a photon index in the range $2 \lesssim \Gamma \lesssim 2.5$ (the interval of values of Γ observed so far in the millisecond pulsar population, Becker & Trümper 1999) does not provide an adequate description of the XMM-Newton and Chandra data.

A simple power-law spectrum can naturally arise also from particles acceleration in a shock and this picture is particularly interesting in the case of the J0737-3039 system, where the relativistic wind from the recycled pulsar A could generate a bow shock at the interface with the insterstellar medium (provided the velocity of the binary through the medium is $\gtrsim 200$ km s^{-1}) or when the wind interacts with the magnetosphere of pulsar B (Granot & Mészáros 2004). On the other hand, both these mechanisms are believed to produce high-energy spectra with $2 \leq \Gamma \leq 3$ (Granot & Mészáros 2004) and a power-law index $\Gamma \gtrsim 3$ (at 90% confidence) appears difficult to accomodate.

A power-law spectrum with $\Gamma = 2$ can model satisfactorily the observed spectrum of J0737–3039 system only if it is combined with a dominant thermal emission: in this case, at a distance of 0.5 kpc, the upper limit to the power-law contribution is at a level of $\sim 4 \times 10^{29}$ erg s^{-1}. The latter luminosity would nicely match the predictions of Granot & Mészáros (2004) for the X–ray emission from a bow shock on the interstellar medium or surrounding pulsar B magnetosphere. But also a simple magnetospheric emission from pulsar A [2] is compatible with that luminosity. In fact, a two-component model (i.e. a thermal emission plus a non-thermal power-law contribution) has been adopted for improving the fit of the spectrum of PSR J0437–4715 (Zavlin et al. 2002), but only a long integration with XMM-Newton can assess if it is required in the case of the J0737–3039 system.

During the refereeing process we became aware of a similar analysis by Pellizzoni et al. (2004). Even if they did not include Chandra data in the analysis they reached similar conlclusions.

[2] It is calculated according to the correlation between the spin-down power $\dot{E}$ of the recycled pulsars in the galactic field and their observed X–ray luminosity L_x, $L_x \propto \dot{E}^{\beta}$ with $\beta = 1.37 \pm 0.10$, Possenti et al. (2002). The scatter around this correlation is about one order of magnitude.

REFERENCES

Arons, J. 1981, ApJ, 248, 1099

Arons, J., Backer, D.C., Spitkovvsky, A. & Kaspi, V.M 2004, in Binary Radio Pulsar, ASP Conf.Ser., ed. F.Rasio & I.Stairs, (astro-ph/0404159)

Becker, W., & Trümper, J. 1999, A&A, 341, 803

Becker, W., & Aschenbach, B. 2002, Proc. of Neutron Stars, Pulsars and Supernova Remnants, MPE Report 278, 64, ed. W. Becker, H. Lesch, & J. Trümper

Burgay, M., D'Amico, N., Possenti, A., Manchester, R. N., Lyne, A. G., Joshi, B. C., McLaughlin, M. A., Kramer, M., Sarkissian, J. M., Camilo, F., Kalogera, V., Kim, C. & Lorimer, D. R. 2003, Nature, 426, 531

Cheng, A.F., & Ruderman, M.A. 1980, ApJ, 235, 576

Cordes, J.M., & Lazio, T.J.W. 2002, preprint (astro-ph/0207156)

Dickey, J.M., & Lockman, F.J. 1990, ARA&A, 28, 215

Harding, A.K., & Muslimov, A.G. 2002, ApJ, 568, 862

Granot, J., & Mészáros, P. 2004, ApJ, 609, L17

Grindlay, J.E., Camilo, F., Heinke, C.O., Edmonds, P.D., Cohn, H., & Lugger, P. 2002, ApJ, 581, 470

Kaspi, V.M., Ransom, S.M., Backer, D.C., Ramachandran, R., Demorest, P., Arons, J., & Spitkovsky, A., 2004, ApJ, submitted (astro-ph/0401161)

Kramer, M., Lyne, A.G., Burgay, M., Possenti, A., Manchester, R.N., Camilo, F., McLaughlin, M.A., Lorimer, D.R., D'Amico, N., Joshi, B.C., Reynolds, J., & Freire, P.C.C. 2004, Proc. of Binary Pulsars, ASP Conf. Ser., ed. F.Rasio & I.Stairs (astro-ph/0405179)

Jenet, A.F., & Ransom, S.M. 2004, Nature, 428, 919

Lorimer, D.R., Burgay, M., Freire, P.C.C., Lyne, A.G., Kramer, M., Possenti, A., McLaughlin, M.A., Camilo, F., Manchester, R.N., D'Amico, N., & Joshi, B.C. 2004, Proc. of Binary Pulsars, ASP Conf. Ser., ed. F.Rasio & I.Stairs (astro-ph/0404274)

Lyne, A. G., Burgay, M., Kramer, M., Possenti, A., Manchester, R. N., Camilo, F., McLaughlin, M. A., Lorimer, D. R., D'Amico, N., Reynolds, J., & Freire, P. C. C. 2004, Science, 303, 1153

Lyutikov, M. 2004, ApJ, submitted (astro-ph/0403076)

Manchester, R.N., Lyne, A.G., Burgay, M., Kramer, M., Possenti, A., Camilo, F., Hotan, A.W., McLaughlin, M.A., Lorimer, D.R., D'Amico, N., Joshi, B.C., Reynolds, J.E., Freire, P.C.C. 2004, Proc. of Binary Pulsars, ASP Conf. Ser., ed. F.Rasio & I.Stairs, in press

McLaughlin, M. A., Camilo, F., Burgay, M., D'Amico, N., Joshi, B.C., Kramer, M., Lorimer, D.R., Lyne, A.G., Manchester, R.N., & Possenti, A. 2004, ApJ, 605, L41

Nicastro, L., Cusumano, G., Loemher, Ö., Kramer, M., Kuiper, L., Hermsen, W., Minee, T., & Becker, W. 2004, A&A, 413, 1065

Pellizzoni, A., et al. 2004, ApJ, in press (astro-ph/0407312)

Ramachandran, R., Backer, D.C., Demorest, P., Ransom, S.M., & Kaspi, V.M. 2004, ApJ, 606, 1167

Ransom, S.M., Kaspi, V.M., Ramachandran, R., Demorest, P., Backer, D.C., Pfahl, E.D., Ghigo, F.D., & Kaplan, D.L. 2004, ApJ, 609, L71

Snowden, S., Immler, S., Arida, M., Perry, B., Still, M., Harrus, I. 2004, The XMM ABC guide, http://heasarc.gsfc.nasa.gov/docs/xmm/abc/

Zavlin, V.E., Pavlov, G.G., Sanwal, D., Manchester, R.N., Trümper, J., Halpern, J.P., & Becker, W. 2002, ApJ, 569, 894

Zhang, B., Loeb, A., 2004, ApJ, submitted (astro-ph/0406609)

TABLE 1
SPECTRAL FITS TO J0737–3039.

Model	Column density (10^{21} cm^{-2})	Ph. Index/ Temperature	$\chi^2_{\rm red}$ (n.h.p.)
Power-law	$1.8^{+1.6}_{-0.7}$	$4.2^{+2.1}_{-1.2}$	0.9 (0.54)
Power-law	< 0.1	2 (fixed)	4.0 (1×10^{-6})
Bremsstrahlung	< 1.0	$0.56^{+0.18}_{-0.19}$ keV	1.0 (0.42)
Black body	< 0.4	$0.20^{+0.02}_{-0.02}$ keV	1.6 (0.07)
NSA	< 0.5	$6.07^{+0.06}_{-0.16}$	1.2 (0.24)
Black+power	< 0.9	$0.16^{+0.04}_{-0.03}$ keV	1.2 (0.28)

The degrees of freedom are 12 for all the models, 13 for the power-law with fixed $\Gamma = 2$ and 11 for the last model in the table.

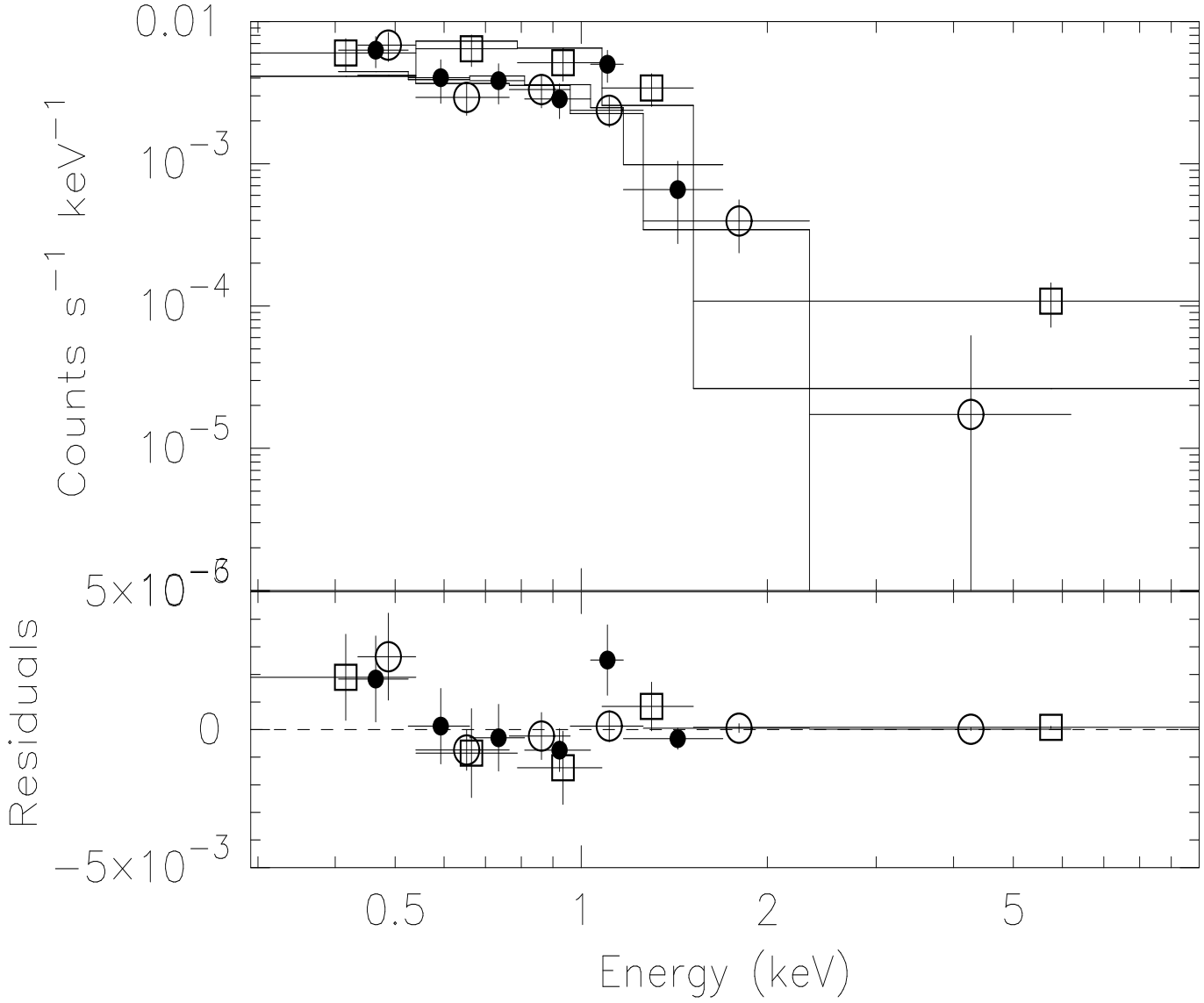

FIG. 1.— Best fit of the pure black body spectrum. Squares indicate Chandra data, filled dots MOS1 data and open dots MOS2 data.

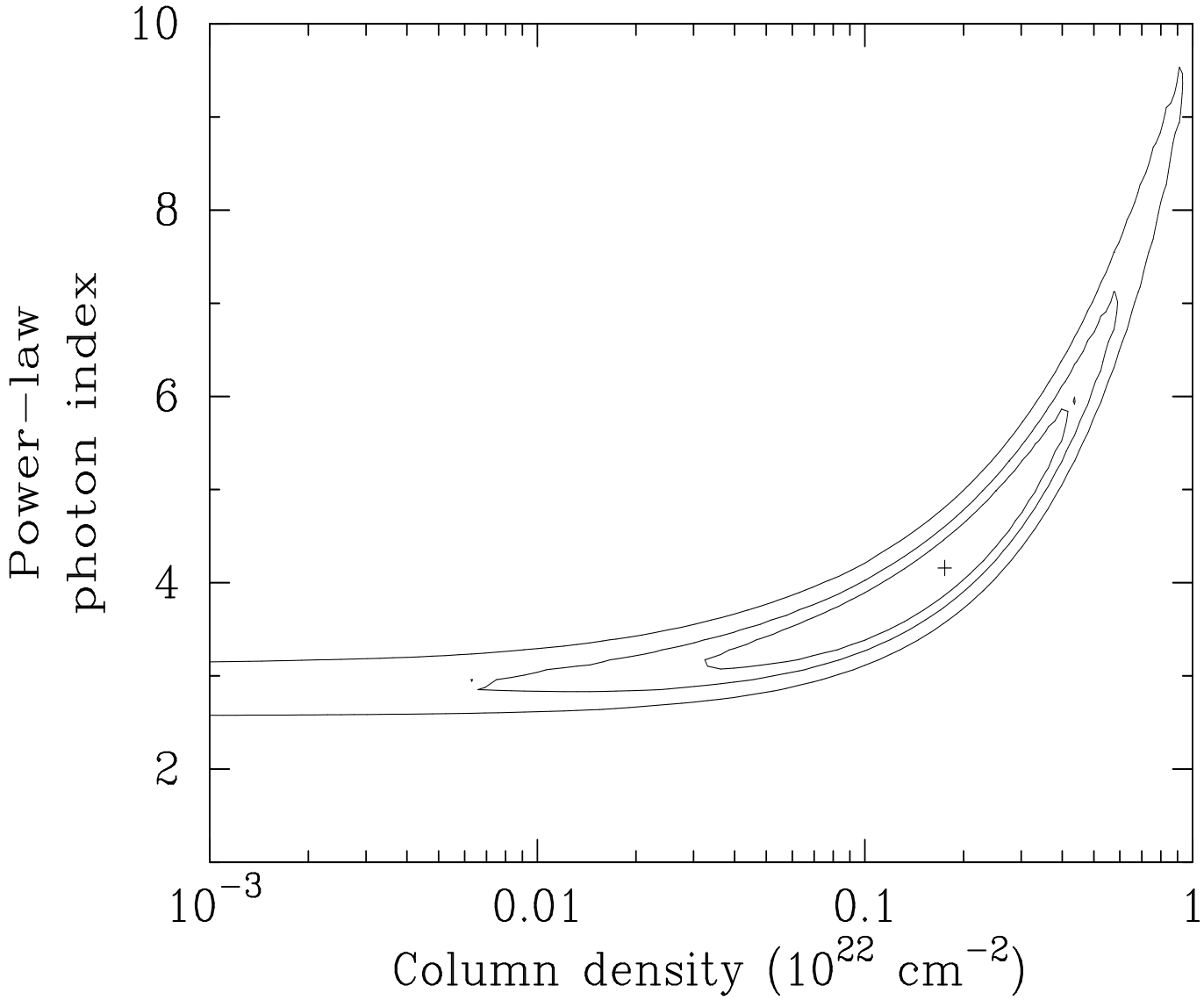

FIG. 2.— Countour plot of the power law fit, ellipses refers to 1, 2 and 3 σ levels. A value of the photon index $\Gamma = 2$ is outside the 3σ contour level. Note that the column density axis is in logaritmic scale.

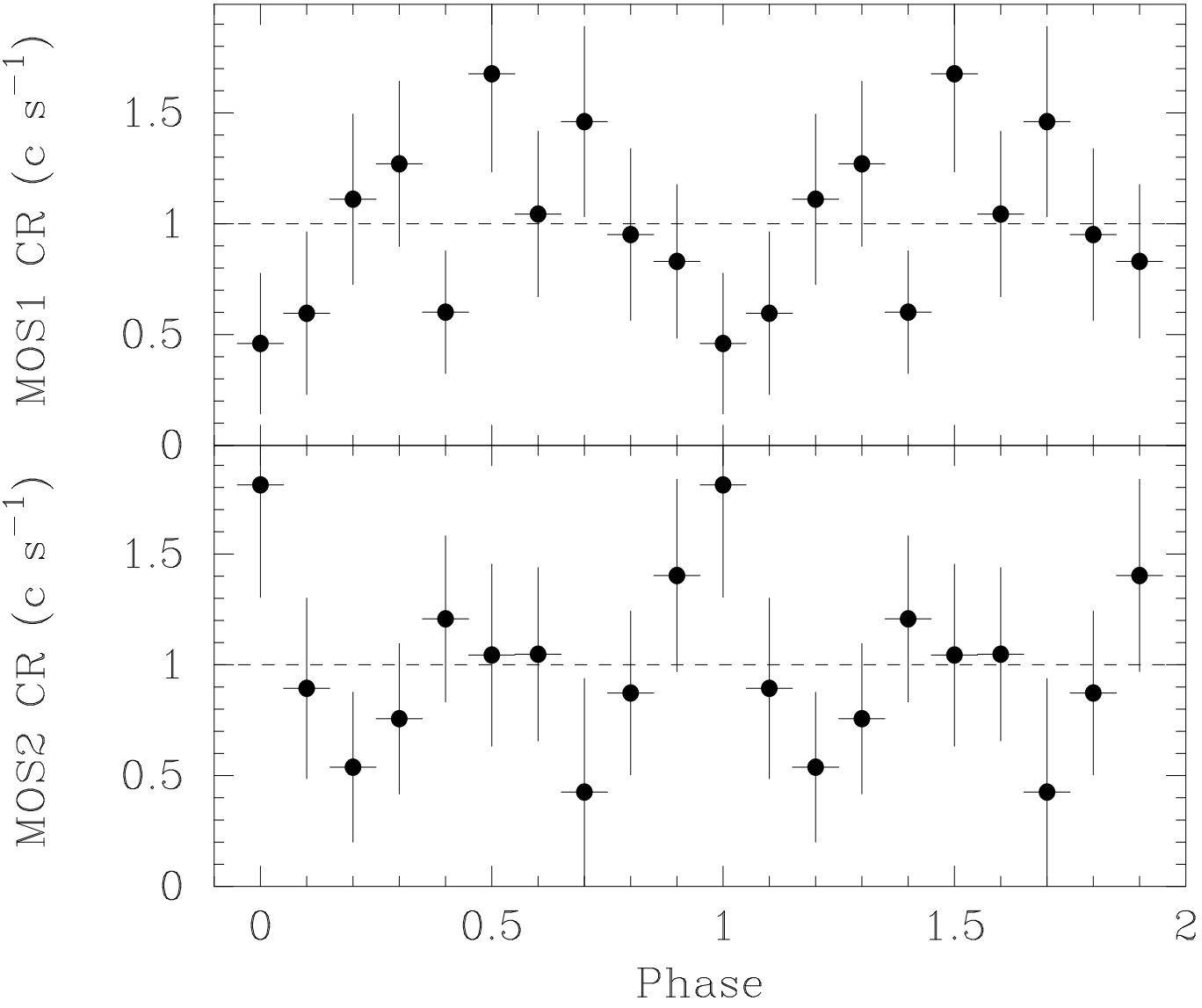

FIG. 3.— MOS1 (upper) and MOS2 (lower) folded background subtracted light curves. Both curves are consistent with a constant emission.